Physica B 457 (2015) 22–29

Contents lists available at ScienceDirect

Physica B

journal homepage: www.elsevier.com/locate/physb

First principles investigations on the mechanical and vibrational properties for the selected B2-AgRE (RE=Sc, Y, La, Ce) intermetallics

C. Çoban [a,*], Y.Ö. Çiftci [b], K. Çolakoglu [b]

[a] Balıkesir University, Department of Physics, Çağış Campus, 10145, Balıkesir, Turkey
[b] Gazi University, Department of Physics, Teknikokullar, 06500, Ankara, Turkey

ARTICLE INFO

Article history:
Received 4 April 2014
Received in revised form
22 September 2014
Accepted 23 September 2014
Available online 2 October 2014

Keywords:
AgRE
Elastic properties
Thermodynamic properties
Lattice dynamics

ABSTRACT

We calculated the lattice constants, bulk modulus and its pressure derivative, elastic constants of B2- based AgRE (RE=Sc, Y, La, Ce) compounds using first principles calculations based on density functional theory (DFT). The elastic properties such as Zener anisotropy factor, Young's modulus, Poisson's ratio, and shear modulus were obtained using the calculated elastic constants. To understand bonding properties, the total charge density and Mulliken charge population were calculated. The phonon dispersion curves and one-phonon density of states were obtained and presented. Also, we presented the temperature variations of various thermodynamic properties such as entropy and heat capacity for the AgRE (RE=Sc, Y, La, Ce). We compared our results for AgRE (RE=Sc, Y, La, Ce) intermetallics with the previous data. Our calculated results for these compounds agree well with the previous theoretical calculations and the experiments.

1. Introduction

The intermetallic alloys development for the structural applications has been an active field of research area around the world. Recently, the intermetallic compounds crystallize in CsCl-type (B2) structure are extremely attractive materials for the high-temperature industrial applications [1–7]. Optimized descriptions of the phase diagram and thermodynamic properties of the Ag–Pr and Ag–Ce systems have been obtained from experimental thermodynamic and phase diagram data by means of the computer program THERMO-CALC based on the least squares method, using models for the Gibbs energy of individual phases by Yin et al. [8,9]. The structural stability of CeAg has been studied by self-consistent full-potential linearized augmented plane wave method (FP-LAPW) based on the density functional theory (DFT) by Zhang et al. [10]. Siethoff has calculated the Debye temperature of CeAg using elastic constants [11]. The lattice constants, formation enthalpies, bulk modulus, elastic constants and electronic structures of B2-based AgRE (RE=Sc, Y and La–Lu) have been calculated by means of first-principles based on the density functional theory by Tao et al. [12]. The lattice constants of AgRE (RE=Ce, Pr) have also been presented by Villars et al. [13]. The experimental elastic constants of AgRE (RE=Ce, Pr) have been reported by Takke [14] and Giraud et al. [15], respectively.

The structural, elastic, phonon properties of B2-AgRE are very important and essential for the material design and the development of new materials. Up to now, to our knowledge, there are little systematic studies on anisotropy, Poisson's ratios, Young's modulus of AgRE (Ag: 0, 0, 0; RE=Sc, Y, La, Ce:1/2, 1/2, 1/2; space group $Pm\bar{3}m$ (221)) intermetallic compounds in B2 structure along crystal directions and there is no study on phonon properties of these compounds. Therefore, we focused our investigations on the detailed mechanical properties and the lattice dynamical properties of the selected AgRE (RE=Sc, Y, La, Ce) intermetallic compounds in B2 structure. Furthermore, the properties including bulk modulus, elastic constants, Young's modulus, Poisson's ratios, anisotropy factors were also studied in a wide range of pressure (0–35 GPa). The Mulliken charge population was also obtained.

2. Method of calculation

All calculations were performed based on the plane-wave pseudopotential density functional theory (DFT) [16,17] by the Vienna ab initio simulation package (VASP) [18–22]. The projector-augmented wave (PAW) method developed by Blöchl [23] implemented within VASP was employed to describe the electron–ion interactions. The effects of exchange correlation interaction were handled by the generalized gradient approximation (GGA)

* Corresponding author. Tel.: +90 266 6121278/1206; fax: +90 266 6121215.
E-mail addresses: cansucoban@yahoo.com (C. Çoban), yasemin@gazi.edu.tr (Y.Ö. Çiftci).

http://dx.doi.org/10.1016/j.physb.2014.09.037
0921-4526/

functional as proposed by Perdew and Wang [24] and the Perdew-Burke-Ernzerhof (PBE) [25] functional. In the structural calculations, a plane-wave basis set with energy cut-off 600.00 eV was used. The cut-off energy value was found to be adequate for the structural and elastic properties. We did not find any significant changes in the key parameters when the energy cut-off increased from 600 to 650 eV. The Brillouin zone was sampled on a $14\times14\times14$ Monkhorst–Pack k-point mesh [26].

3. Results and discussion

3.1. Structural properties

By taking a series of different lattice parameters a we carried out total energy E calculations over a wide range of primitive cell volumes V. By fitting the calculated E–V results to the Murnaghan EOS [27] (see Fig. 1), we obtained the equilibrium a parameter, bulk modulus B, and first pressure derivative of bulk modulus B' for AgRE (RE=Sc, Y, La, Ce) compounds in B2 structure. The calculated results for GGA and PBE were presented in Table 1. The pressure dependent behavior of a and B were also investigated (see Table 1). For GGA, the calculated a values are in good agreement with experimental and other theoretical data and B values are 5.73%, 6.73%, 6.75%, and 8.53% lower than the other theoretical data given in Ref. [12] for AgRE (RE=Sc, Y, La, Ce), respectively. Besides, the deviation of calculated B values are very small from the previous experimental results given in the Refs. [28] for AgY, [29] for AgLa, and [14] for AgCe. It can be seen that, a decreases whereas B increases with the pressure. For PBE, to our knowledge there are no previous results in the literature.

3.2. Elastic properties

The elastic constants are important parameters which are very important for the determination of strength of the materials. By using them, we can also provide information on the stability of crystal structures. Zener anisotropy factor, shear modulus, Young's modulus, Poisson's ratio, sound velocity, hardness of the materials are related to the elastic constants. In this study, the second-order elastic constants (C_{11}, C_{12}, and C_{44}), listed in Table 1 for GGA and PBE, for B2 structure of AgRE (RE=Sc, Y, La, Ce) were calculated using the "stress-strain" relations [30]. The well known Born–Huang stability criteria on the elastic constants are known as $C_{11}-C_{12}>0$, $C_{11}>0$, $C_{44}>0$, $C_{11}+2C_{12}>0$. It is obvious that, they obey this criteria and also obey the cubic stability condition: $C_{12}<B<C_{11}$ at zero pressure, suggesting that B2 structure of AgRE (RE=Sc, Y, La, Ce) compounds are mechanically stable. The calculated elastic constants given for GGA and PBE are consistent with the other theoretical results taken from the Ref. [12] for all compounds. And, they also agree with experimental results given in the Refs. [28,29], and [14] for AgY, AgLa, and AgCe, respectively.

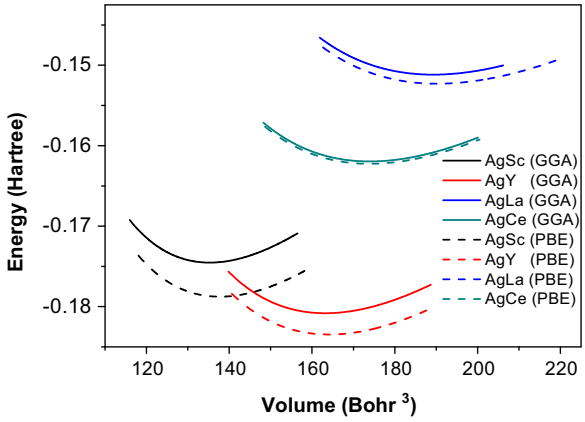

Fig. 1. The total energy-volume graphs for B2 structure of AgRE (RE=Sc, Y, La, Ce).

The effect of pressure on elastic constants was also investigated and the results between 5 and 35 GPa were also presented in Table 1 for these compounds. All calculated elastic constants increase with the pressure but these compounds do not satisfy all the stability criteria under high pressures (at $P=35$ GPa for AgSc and AgY, from $P=10$ GPa for AgLa and AgCe) suggesting that these compounds become mechanically unstable with the pressure.

According to the Johnson [31] and Pettifor [32], the angular character of atomic bonding in metals and compounds could be described by the Cauchy pressure (C_{12}–C_{44}). If the bonding in character is metallic, the Cauchy pressure is typically positive. On the other hand, for directional bonding with angular character, the Cauchy pressure is negative. The calculated C_{12}–C_{44} values are positive at all pressures. We can say that AgRE (RE=Sc, Y, La, Ce) have metallic bonding character.

For the specific case of the cubic lattices, the isotropic shear modulus (G) is calculated using the relations given below [33]:

$$G=\frac{1}{2}(G_V+G_R), \tag{1}$$

where G_V is Voigt's shear modulus ($G_V=(C_{11}-C_{12}+3C_{44})/5$) and G_R is Reuss's shear modulus ($5/G_R=4/(C_{11}-C_{12})+3/C_{44}$). The calculated G values are consistent with the previous results of Ref. [12] for AgRE (RE=Sc, Y, La, Ce) compounds.

The ductile/brittle properties of metals could be related to their elastic constants according to the criterion which has proposed by Pugh [34]. If the ratio of $B/G<1.75$ a material behaves in a brittle, and if it is higher than 1.75 a material behaves in a ductile manner. In our case, B/G value for AgRE (RE=Sc, Y, La, Ce) compounds at zero pressure, listed in Table 2, are higher than 1.75 indicating that the AgRE (RE=Sc, Y, La, Ce) compounds have ductile character in nature.

The anisotropy of the crystal are derived from elastic constants using the following relations [35]:

$$A^{[001],(100)}=\frac{2C_{44}}{C_{11}-C_{12}}, \tag{2}$$

$$A^{[001],(110)}=\frac{C_{44}(C_l+2C_{12}+C_{11})}{C_{11}C_l-C_{12}^2}, \tag{3}$$

where $C_l=C_{44}+(C_{11}+C_{12})/2$ the [ijk] and (ijk) denote symmetry axis and plane, respectively. The anisotropy factor A greater or smaller than 1 is a pointer of the degree of elastic anisotropy in solids. It takes the value of 1 for the completely isotropic material. At zero pressure, the calculated $A^{[001],(100)}$ and $A^{[001],(110)}$ values, given in Table 2 for GGA and PBE, show that these compounds are elastically anisotropic in nature. The $A^{[001],(100)}$ value of AgRE (RE=Sc, La, Ce) for GGA is 3.4%, 7.3%, 31.8% higher than the other theoretical value [12], respectively. For AgY, it is in excellent agreement with this data and 13.85% higher than the other theoretical result and 3.89% lower than the previous experimental data presented in Ref. [28]. Besides, it is also 11.81% higher than experimental value given in Ref. [29] for AgLa. Finally, for AgCe, $A^{[001],(100)}$ value is 40.1% higher than experimental value in Ref. [14]. The $A^{[001],(100)}$ values for PBE agree with the experimental data from literature [28] and [29]. But for AgCe, it is 62.72% higher than the data given in Ref. [14]. The $A^{[001],(100)}$ values calculated using GGA increase with the pressure for AgSc and AgY compounds. However, due to the negative C_{11}–C_{12} values at higher pressures the $A^{[001],(100)}$ values for AgLa and AgCe do not exhibit stable

Table 1
Calculated lattice constants (a), bulk modulus (B), pressure derivative of bulk modulus (B'), and elastic constants (C_{ij}) (in GPa unit) of AgRE (RE=Sc, Y, La, Ce) in B2 structure along with the available experimental and other theoretical data.

Materials	P	Reference	a (Å)	B (GPa)	B'	C_{11}	C_{12}	C_{44}
AgSc	0	This work$^{(GGA)}$	3.422	77.68	4.12	109.8	72.6	44.8
		This work$^{(PBE)}$	3.443	79.62	4.58	109.6	69.0	46.5
		Experiment[a]	3.412					
		Theory [b]	3.436	82.40		106.6	70.2	42.4
	5	This work$^{(GGA)}$	3.368	98.28		126.5	87.9	52.2
		This work$^{(PBE)}$	3.380	99.49		125.7	85.4	55.1
	10	This work$^{(GGA)}$	3.316	116.90		144.2	105.6	59.9
		This work$^{(PBE)}$	3.331	115.10		143.4	100.9	62.5
	15	This work$^{(GGA)}$	3.274	139.48		159.6	122.3	68.8
		This work$^{(PBE)}$	3.289	138.60		157.3	115.7	69.3
	20	This work$^{(GGA)}$	3.238	153.70		173.0	137.9	72.6
		This work$^{(PBE)}$	3.254	143.50		169.9	130.3	75.5
	25	This work$^{(GGA)}$	3.206	180.68		186.4	154.1	78.5
		This work$^{(PBE)}$	3.223	178.70		181.3	149.3	76.3
	30	This work$^{(GGA)}$	3.178	189.10		198.4	168.8	83.5
		This work$^{(PBE)}$	3.194	182.60		193.0	158.3	86.6
	35	This work$^{(GGA)}$	3.153	221.88		210.6	184.0	88.6
		This work$^{(PBE)}$	3.168	220.75		203.8	171.9	91.6
AgY	0	This work$^{(GGA)}$	3.642	63.80	3.95	100.6	52.7	35.5
		This work$^{(PBE)}$	3.649	66.25	4.43	100.5	52.3	36.1
		Experiment[a]	3.6196					
		Theory [b]	3.644	68.4		98.3	53.5	33.6
		Theory [c]	3.634	69.0		105.0	50.0	37.0
		Experiment [c]	3.619	70.5		102.4	54.0	37.2
	5	This work$^{(GGA)}$	3.571	83.55		117.7	66.9	43.5
		This work$^{(PBE)}$	3.572	84.48		118.6	67.4	44.7
	10	This work$^{(GGA)}$	3.506	101.12		133.4	82.6	51.6
		This work$^{(PBE)}$	3.512	98.78		132.8	81.7	52.2
	15	This work$^{(GGA)}$	3.456	123.05		145.4	97.4	58.6
		This work$^{(PBE)}$	3.463	112.23		144.7	95.9	58.9
	20	This work$^{(GGA)}$	3.408	135.79		156.9	114.7	66.1
		This work$^{(PBE)}$	3.420	126.29		147.3	113.7	67.1
	25	This work$^{(GGA)}$	3.375	162.55		164.7	127.6	71.3
		This work$^{(PBE)}$	3.383	152.35		157.8	130.5	69.8
	30	This work$^{(GGA)}$	3.334	169.01		175.4	146.4	78.5
		This work$^{(PBE)}$	3.351	160.81		167.68	144.69	75.5
	35	This work$^{(GGA)}$	3.314	185.05		180.6	156.1	82.1
		This work$^{(PBE)}$	3.321	183.67		178.9	151.7	81.9
AgLa	0	This work$^{(GGA)}$	3.824	48.77	3.96	63.5	46.9	21.9
		This work$^{(PBE)}$	3.833	49.90	4.24	61.9	45.7	22.1
		Experiment[a]	3.814					
		Theory [b]	3.826	52.3		64.5	46.2	22.6
		Experiment[d]		48.6		60.1	42.9	20.4
	5	This work$^{(GGA)}$	3.725	68.57		73.7	64.0	27.7
		This work$^{(PBE)}$	3.737	66.32		72.4	63.2	28.1
	10	This work$^{(GGA)}$	3.645	85.71		83.9	82.4	33.5
		This work$^{(PBE)}$	3.652	84.74		81.9	80.2	33.6
	15	This work$^{(GGA)}$	3.585	108.17		92.7	98.4	38.5
		This work$^{(PBE)}$	3.588	107.62		90.63	96.0	37.8
	20	This work$^{(GGA)}$	3.527	119.75		102.4	116.1	44.3
		This work$^{(PBE)}$	3.537	119.65		99.27	111.8	43.9
	25	This work$^{(GGA)}$	3.492	147.17		108.7	127.9	48.4
		This work$^{(PBE)}$	3.494	142.74		106.7	126.2	48.8
	30	This work$^{(GGA)}$	3.441	152.29		118.7	147.5	54.9
		This work$^{(PBE)}$	3.455	150.82		113.8	140.5	53.6
	35	This work$^{(GGA)}$	3.423	187.37		122.6	155.4	57.6
		This work$^{(PBE)}$	3.424	185.21		120.4	153.9	58.1
AgCe	0	This work$^{(GGA)}$	3.818	50.40	4.3	60.7	48.8	23.8
		This work$^{(PBE)}$	3.826	51.30	4.2	58.6	47.6	25.7
		Experiment[a]	3.75					
		Theory[b]	3.814	55.1		65.5	49.9	23.8
		Experiment[e]		49.6		59.6	44.6	21.5
	5	This work$^{(GGA)}$	3.714	71.70		74.6	67.1	31.3
		This work$^{(PBE)}$	3.732	68.16		73.9	66.8	34.3
	10	This work$^{(GGA)}$	3.639	92.90		88.1	84.3	38.4
		This work$^{(PBE)}$	3.645	89.22		87.3	83.6	42.4
	15	This work$^{(GGA)}$	3.581	114.30		99.8	100.1	45.0
		This work$^{(PBE)}$	3.614	105.70		96.4	93.0	47.3
	20	This work$^{(GGA)}$	3.534	135.60		110.0	115.0	51.1
		This work$^{(PBE)}$	3.552	134.50		108.6	112.8	54.7
	25	This work$^{(GGA)}$	3.493	156.90		119.5	129.1	56.8
		This work$^{(PBE)}$	3.519	160.70		114.6	123.7	58.2

Table 1 (*continued*)

Materials	P	Reference	a (Å)	B (GPa)	B′	C_{11}	C_{12}	C_{44}
	30	This work$^{(GGA)}$	3.459	178.20		128.2	142.9	62.1
		This work$^{(PBE)}$	3.482	176.90		125.2	139.6	64.3
	35	This work$^{(GGA)}$	3.428	199.50		136.5	156.5	66.9
		This work$^{(PBE)}$	3.432	197.90		134.9	152.1	67.7

[a] Ref. [13].
[b] Ref. [12].
[c] Ref. [28].
[d] Ref. [29].
[e] Ref. [14].

Table 2
Calculated elastic anisotropy (A), Poisson's ratio (σ), Young's modulus (Y) (in GPa), shear modulus (G) (in GPa), and B/G ratio for B2 phase of AgRE (RE=Sc, Y, La, Ce) at zero pressure with the available experimental and other theoretical data.

Materials	Reference	A	$A^{[001],(100)}$	$A^{[001],(110)}$	σ	$\sigma^{[001]}$	$\sigma^{[111]}$	Y	$Y^{[001]}$	$Y^{111]}$	G	B/G
AgSc	This work$^{(GGA)}$		2.41	1.81		0.39	0.27		51.94	114.52	31.5	2.46
	This work$^{(PBE)}$		2.32	1.76		0.38	0.26		56.27	117.57	33.1	2.41
	Theory[a]	2.33			0.336			80.8			30.2	
AgY	This work$^{(GGA)}$		1.48	1.33		0.34	0.28		64.4	90.9	30.3	2.10
	This work$^{(PBE)}$		1.49	1.34		0.34	0.275		64.7	92.0	30.7	2.16
	Theory[a]	1.50			0.317			75.2			28.6	
	Theory[b]	1.3			0.32							
	Experiment[b]	1.54			0.345							
AgLa	This work$^{(GGA)}$		2.65	1.91		0.42	0.31		23.5	57.7	14.8	3.29
	This work$^{(PBE)}$		2.72	1.94		0.42	0.31		23.1	57.9	14.8	3.37
	Theory[a]	2.47			0.363			42.8			15.7	
	Experiment[c]	2.37										
AgCe	This work$^{(GGA)}$		4.02	2.37		0.445	0.304		17.1	62.1	13.7	3.68
	This work$^{(PBE)}$		4.67	2.54		0.44	0.3		19.28	66.06	14.0	3.66
	Theory[a]	3.05			0.373			41.8			15.2	
	Experiment[d]	2.87										

[a] Ref. [12].
[b] Ref. [28].
[c] Ref. [29].
[d] Ref.[14].

character. Therefore, the pressure dependence of $A^{[001],(100)}$ values are presented only for AgSc and AgY (see Fig. 2a). The pressure dependence of $A^{[001],(100)}$ values for these compounds calculated for PBE are also plotted in Fig. 2a. The $A^{[001],(100)}$ values for GGA and PBE almost coincide at low pressures. However, the difference between them increases with the pressure.

The $A^{[001],(110)}$-pressure graph is depicted in Fig. 2b for GGA and PBE which shows that they increase with pressure. The $A^{[001],(110)}$ values calculated for GGA and PBE are smaller than $A^{[001],(100)}$ and experimental data taken from the Refs. [14,28,29] for AgRE (RE=Y, La, Ce).

The Young's modulus Y is defined as the ratio between tensile stress and tensile strain and is an indicator of the stiffness of the solid, i.e., if the value of Y is larger, the material is stiffer. The Young's modulus Y for [001] and [111] directions may be expressed in terms of the elastic constants [36]:

$$Y^{[001]} = \frac{(C_{11}-C_{12})(C_{11}+2C_{12})}{C_{11}+C_{12}}, \tag{4}$$

$$Y^{[111]} = \frac{3C_{44}(C_{11}+2C_{12})}{C_{11}+2C_{12}+C_{44}}. \tag{5}$$

At zero pressure, the calculated $Y^{[001]}$ and $Y^{[111]}$ values of AgRE (RE=Sc, Y, La, Ce) are given in Table 2 for GGA and PBE. We can say that this shows the clear bonding nature in [001] and [111] directions, and appears anisotropy in these compounds. For these functionals, the pressure dependent behavior of the $Y^{[001]}$ and $Y^{[111]}$ of AgRE (RE=Sc, Y, La, Ce), along [001] and [111] directions were plotted in Fig. 3a and b, respectively. It can also be seen that the effect of pressure on the $Y^{[001]}$ and $Y^{[111]}$ values is different, i.e., the Young's modulus increases with pressure along [111] direction almost linearly for all compounds for both GGA and PBE, while the Young's modulus decreases nonlinearly for AgY and AgSc and almost linearly for AgCe and AgLa with pressure along [001] direction. The $Y^{[001]}$ values are smaller while $Y^{[111]}$ values are higher than other theoretical results given in Ref. [12] for all compounds.

The Poisson's ratio σ provides more information about the characteristics of the bonding forces than the other elastic properties [37] which depends most strongly on changes in inter-atomic bonding type. The lower and upper limit of σ are 0.25 and 0.5 for central forces in solids which correspond to incompressible solid [38]. The σ of the crystals were calculated using the following relations [36]:

$$\sigma^{[001]} = \frac{C_{12}}{C_{11}+C_{12}}, \tag{6}$$

$$\sigma^{[111]} = \frac{C_{11}+2C_{12}-2C_{44}}{2(C_{11}+2C_{12}+C_{44})}. \tag{7}$$

The pressure dependence of the σ values of AgRE (RE=Sc, Y, La, Ce) along the [001] and [111] directions was plotted in Fig. 4a,b for

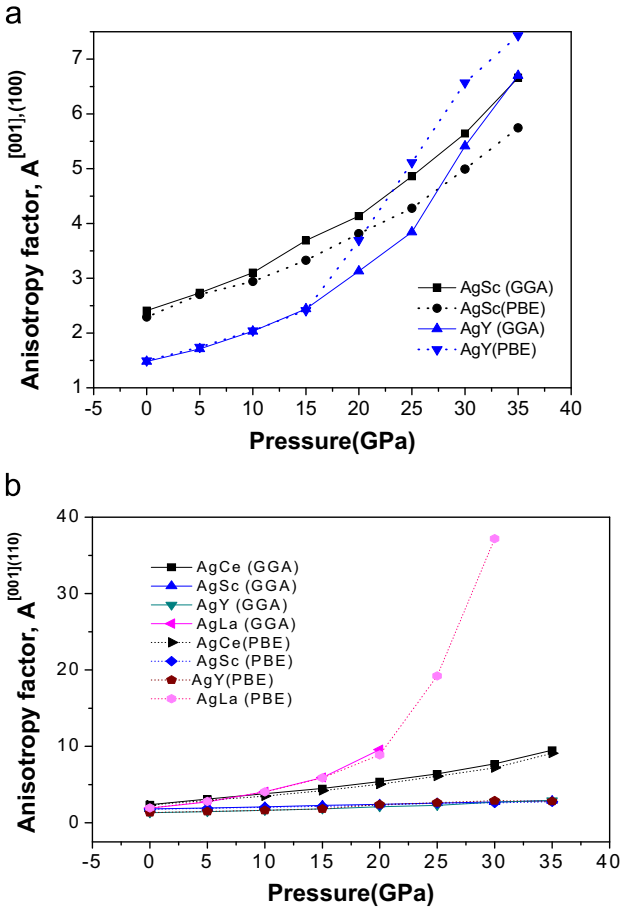

Fig. 2. The pressure dependence of (a) Anisotropy factor$^{[001],\ (100)}$ (b) Anisotropy factor$^{[001],\ (110)}$ for B2 structure of AgRE (RE=Sc, Y, La, Ce).

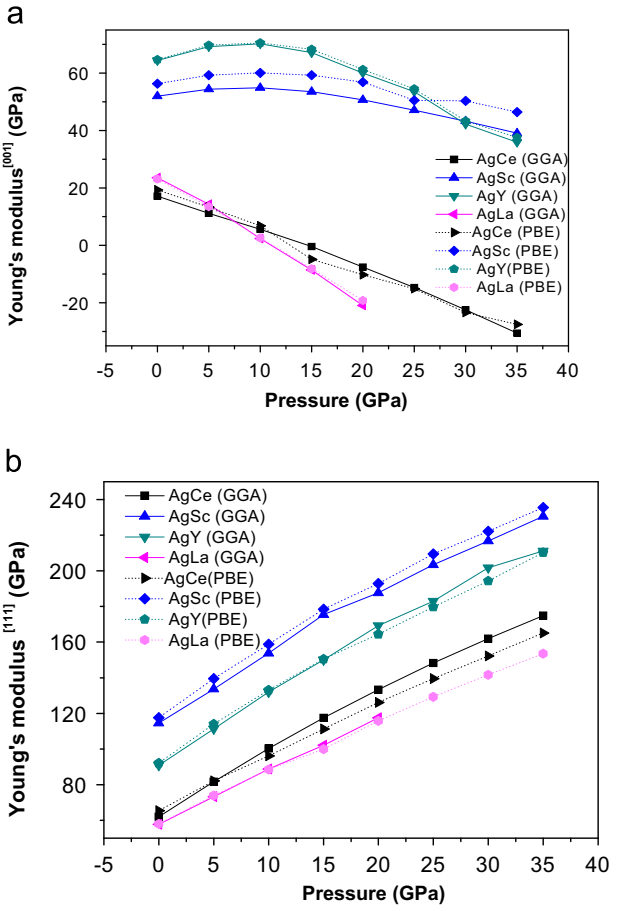

Fig. 3. The pressure dependence of (a) Young's modulus$^{[001]}$ (b) Young's modulus$^{[111]}$ for AgRE (RE=Sc, Y, La, Ce) in B2 structure.

GGA and PBE. As can be seen from the Table 2, the calculated $\sigma^{[001]}$ and $\sigma^{[111]}$ values are the same/almost the same for both functional at zero pressure i.e. for this phase, the forces in these compounds are central. At high pressures, there is no a clear difference between the $\sigma^{[001]}$ values calculated for GGA and for PBE. The values of $\sigma^{[001]}$ increase rapidly with increasing pressure at the beginning, from 15 GPa it increases almost linearly for AgCe. It increases almost linearly for AgSc, AgY and for AgLa with increasing pressure (see Fig. 4a). The $\sigma^{[111]}$ values of AgCe increase with pressure at 0–10 GPa and 30–35 GPa, but from 15 to 30 GPa it starts to decrease. For AgLa and AgSc, it increases with increasing pressure. For AgY, it almost remains constant at 0–15 GPa, but for $P > 15$ GPa it starts to increase. The calculated σ values are consistent with the other available theoretical results (given in Ref. [12]) for all compounds and experimental data presented in Ref. [28] for AgY.

3.3. Bonding behavior

The Mulliken charge population was performed for B2 phase of AgRE (RE=Sc, Y, La, Ce) compounds to understand bonding behavior. The calculated results are presented in Table 3. For AgRE (RE=Sc, Y, La, Ce) the charge transfer from RE=Sc, Y, La, and Ce atoms to Ag are found as 0.61e, 0.23e, 0.93e, and 0.86e, respectively. These values are smaller than the charge population in Ag and RE=Sc, Y, La, Ce atoms. Therefore, we decided that the bonding behavior of B2 of phase AgRE (RE=Sc, Y, La, Ce) is a combination of stronger ionic and weaker covalent character. The RE=Sc, La, Ce 2p, the Y and Ag 4d orbits are conduced largely to the charge population. This result is compatible with the calculated positive Cauchy pressure ($C_{12}-C_{44}$) which supports the metallic bonding. The total charge density for B2 phase of the selected AgCe compound was also displayed in Fig. 5 which indicates an ionic bonding between Ag and Ce atoms. Therefore, we concluded that the general bonding behavior of AgCe is a combination of metallic, ionic, and weak covalent characters.

3.4. Phonon properties

The phonon dispersion curves and one-phonon DOS for B2 phase of AgRE (RE=Sc, Y, La and Ce) were calculated using GGA and PBE along the high symmetry directions using a $2\times2\times2$ supercell approach (see Fig. 6(a–d)) by the PHONOPY code [39]. This code was based on the forces obtained from the VASP. It calculates force constant matrices and phonon frequencies using the "Super lattice Approximation Method" as described in References [40]. Generally, if the GGA results are compared with the data calculated using PBE, it can be seen from the PBE results that the R symmetry point shifts to the left (to the M symmetry point). In the phonon dispersion curves, a clear gap between optic and acoustic modes is observed due to the small mass ratio of constituent atoms (cation and anion) for GGA result of AgLa and for PBE result of AgSc compounds. On the other hand, there is no a clear gap between optic and acoustic modes in the phonon spectra of the other compounds for the

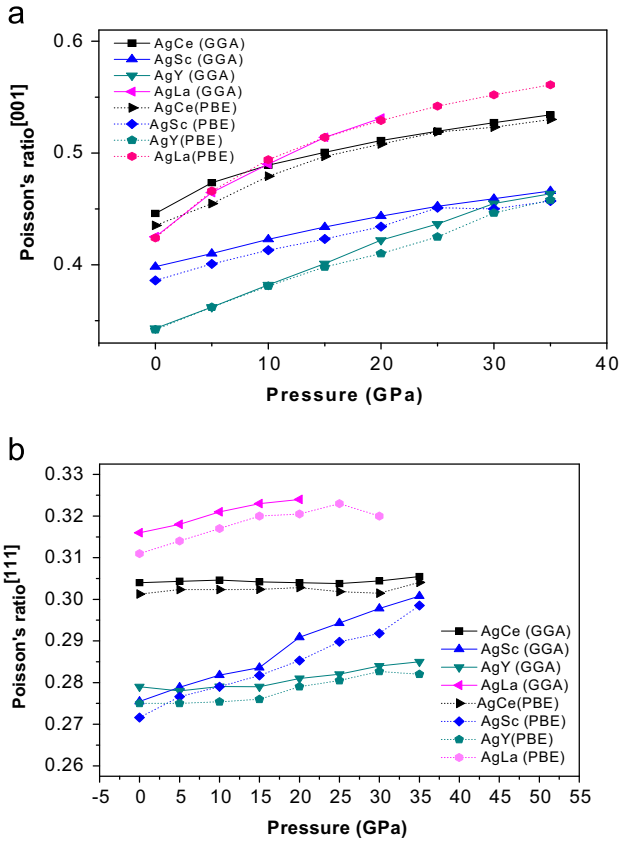

Fig. 4. The pressure dependent behavior of (a) Poisson's ratio$^{[001]}$ (b) Poisson's ratio$^{[111]}$ for AgRE (RE=Sc, Y, La, Ce) in B2 structure.

Table 3
The Mulliken charge population of AgRE (RE=Sc, Y, La, Ce) in B2 structure.

Materials	Species	Reference	Charge Populations					
			s	p	d	f	Total	Charge (e)
AgSc	Ag	This work	0.78	1.14	9.69	0.00	11.61	−0.61
	Sc		2.24	6.65	1.51	0.00	10.39	0.61
AgY	Ag	This work	0.56	0.84	1.83	0.00	3.23	−0.23
	Y		0.95	0.09	9.73	0.00	10.77	0.23
AgLa	Ag	This work	1.06	1.11	9.77	0.00	11.93	−0.93
	La		2.02	6.11	1.94	0.00	10.07	0.93
AgCe	Ag	This work	0.98	1.16	9.72	0.00	11.86	−0.86
	Ce		2.19	5.93	1.87	1.14	11.14	0.86

calculated results using both GGA and PBE. The absence of imaginary frequencies (soft phonon modes) in the phonon dispersion curves strongly supports the dynamically stable character for the B2 structure of AgRE (RE=Sc, La). But, the vibrational anomaly is seen in phonon dispersion spectra for GGA calculation of AgY and for the calculation with PBE of AgCe which contains soft modes at M symmetry points in BZ. Unfortunately, there is no experimental and other theoretical works on the lattice dynamics of these compounds in literature for comparison with the present data. The related one-phonon density of states are also shown for these compounds.

3.5. Temperature dependency of entropy and heat capacity

Using the phonon frequencies and DOS data obtained from VASP and PHONOPY codes, the temperature dependent variations of the entropy S and heat capacity at constant volume C_v were

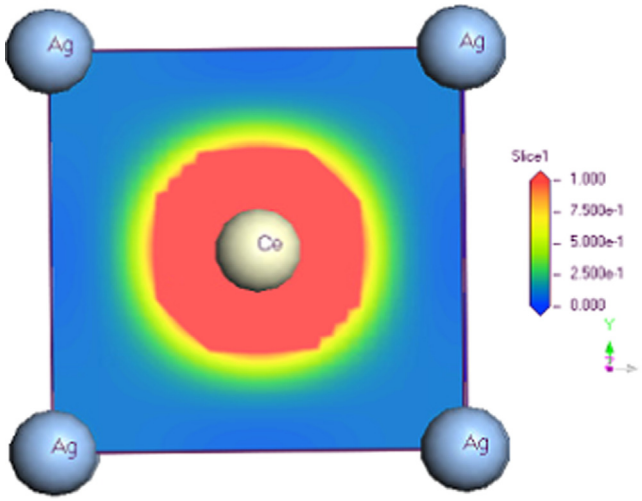

Fig. 5. The electron charge density distributions for the AgCe.

calculated by GGA and PBE for AgRE (RE=Sc, Y, La, Ce) compounds which are given in Fig. 7a, b.

The calculated S values using the PBE functional are higher than that are found for GGA. On the other hand, there is no clear difference between the temperature dependence behavior of GGA and PBE results (see Fig. 7a). For both functionals, entropies increase with the temperature. Additionally, the entropy value of AgCe for GGA and of AgLa for PBE has the higher values than the others. Obviously, the entropy curves exhibit a similar trend with heat capacity.

The temperature dependence of heat capacity for AgRE (RE=Sc, Y, La, Ce) compounds are illustrated in Fig. 7b. For decreasing the probable influence of anharmonicity, the temperature is limited to 500 K. It is interesting to note that, the heat capacity curve of AgRE (RE=Sc, Y, La) approaches to each other for GGA. But for PBE, the calculated values exhibit almost the same character in 0–500 K. The contribution from the lattice vibrations to the heat capacity follows the Debye model and approaches the Dulong-Petit limit at high temperatures as shown in Fig. 7 b illustrating that the anharmonic effects are suppressed.

4. Summary and conclusion

In this study, we investigated the structural, elastic and vibrational properties of AgRE (RE=Sc, Y, La, Ce) using the plane-wave pseudopotential approach to the density functional theory using GGA and PBE. The optimized lattice constants for GGA are in good agreement with the other experimental and theoretical values. Our results for elastic constants satisfy the traditional mechanical stability conditions at zero pressure. The Mulliken charge population was performed. The calculated phonon dispersion curves do not contain soft modes at any direction for AgSc and AgLa for both GGA and PBE, which confirms the stability of the B2 structure of these compounds. But, the soft phonon modes were observed in phonon dispersion spectra of AgY for GGA and of AgCe for PBE and this structure is dynamically unstable due to the existing of imaginary frequencies at 0 GPa for these compounds. It is hoped that some of our results, such as the pressure dependence of structural and elastic properties, and phonon dispersion curves of AgRE (RE=Sc, Y, La, Ce) in B2 structure estimated for the first time in this work will be tested in future experimentally and theoretically.

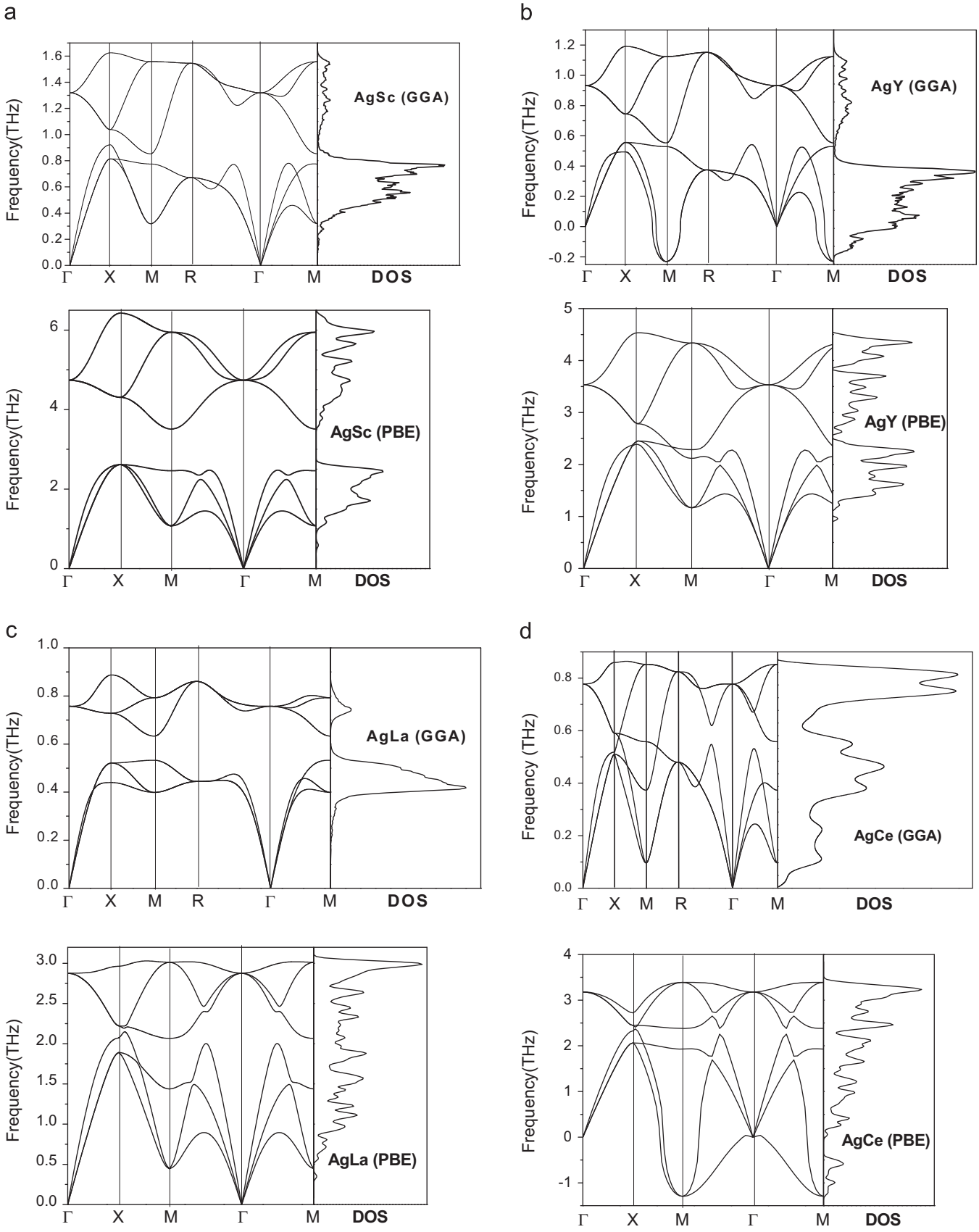

Fig. 6. Calculated phonon dispersion curves and one-phonon density of states for (a) AgSc (b) AgY (c) AgLa (d) AgCe in B2 structure.

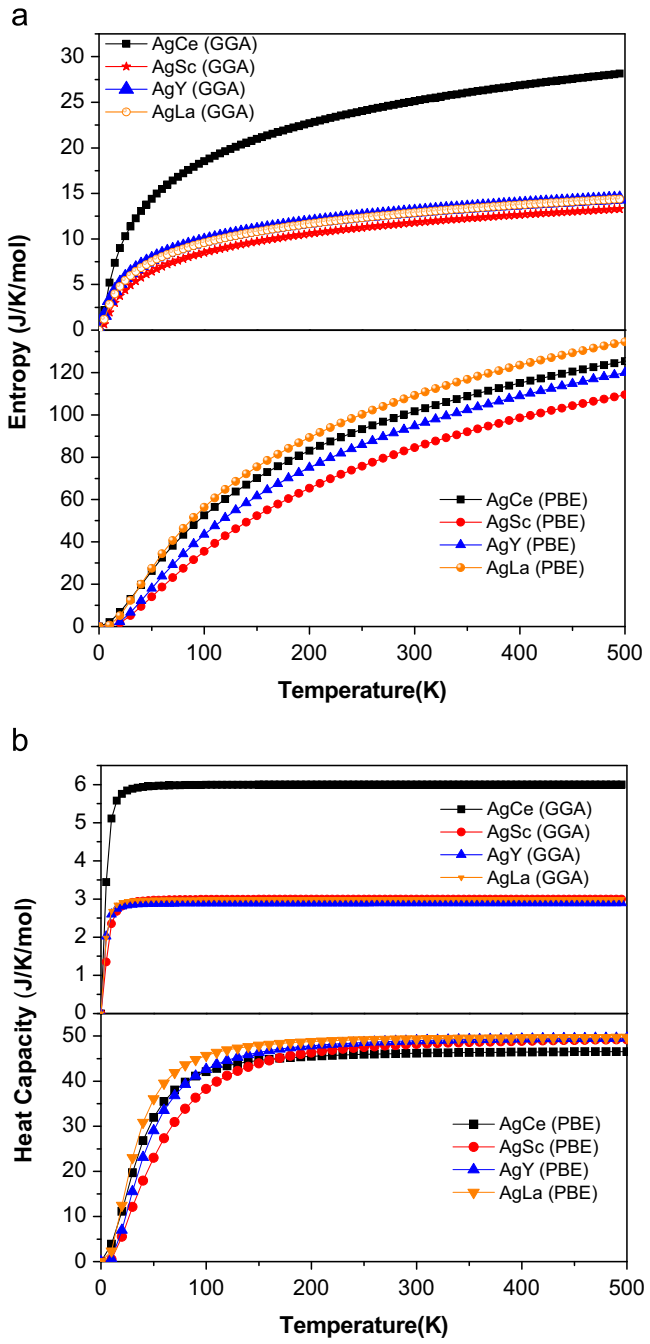

Fig. 7. The temperature dependence of (a) entropy (b) heat capacity for AgRE (RE=Sc, Y, La, Ce) in B2 structure.

Acknowledgments

This work is supported by Balıkesir University Research Project Unit under Project No: 2012/13 and Gazi University Research Project Unit under Project No: 05/2010-51.

References

[1] C.T. Liu, E.P. George, P.J. Maziasz, J.H. Schneibel, Mater. Sci. Eng. A 258 (1998) 84.
[2] I. Baker, Mater. Sci. Eng. A 192/193 (1995) 1.
[3] N.S. Stoloff, C.T. Liu, S.C. Deevis, Intermetallics 8 (2000) 1313.
[4] D.B. Miracle, Acta Metall. Mater 41 (1993) 649.
[5] B.L. Mordike, Mater. Sci. Eng. A 324 (2002) 103.
[6] B.L. Mordike, J. Mater. Process.Technol. 117 (2001) 381.
[7] G.W. Lorimer, P.J. Apps, H. Karimzaden, J.F. King, Mater. Sci. Forum 279 (2003) 419.
[8] F. Yin, X. Su, Z. Li, P. Zhang, M. Huang, Y. Shi, J. Alloys Comp 307 (2000) 202.
[9] F. Yin, M. Huang, X. Su, P. Zhang, Z. Li, Y. Shi, J. Alloys Comp 334 (2002) 154.
[10] Y.S. Zhang, K.L. Yao, Z.L. Liu, Solid State Commun. 134 (2005) 343.
[11] H. Siethoff, Intermetallics 5 (1997) 625.
[12] X. Tao, H. Chen, X. Li, Y. Ouyang, S. Liao, Phys. Scr. 83 (2011) 045301.
[13] P. Villars, L.D. Calvert, Pearson's Handbook of Crystallographic Data for Intermetallic Phases, vol 1–4, ASM International, Materials Park, OH, 1991.
[14] R. Takke, N. Dolezal, W. Assmus, B. Lüthi, J. Magn. Magn. Mater. 23 (1981) 247.
[15] M. Giraud, P. Morin, J. Rouchy, D. Schmitt, E du Trémolet de Lacheisserie, J. Magn. Magn. Mater. 37 (1983) 83.
[16] P. Hohenberg, W. Kohn, Phys. Rev. B 136 (1964) 384.
[17] W. Kohn, L.J. Sham, Phys. Rev. A 140 (1965) 1133.
[18] G. Kresse, J. Hafner, Phys. Rev. B 47 (1993) 558.
[19] G. Kresse, J. Hafner, J. Phys.: Condens. Matter 6 (1994) 8245.
[20] G. Kresse, J. Hafner, Phys. Rev. B 49 (1994) 14 251.
[21] G. Kresse, J. Furthmüller, Comput. Mater. Sci. 6 (1996) 15.
[22] G. Kresse, J. Furthmüller, Phys. Rev. B 54 (1996) 11 169.
[23] P.E. Blöchl, Phys. Rev. B 50 (1994) 17 953.
[24] J.P. Perdew, Y. Wang, Phys. Rev. B 45 (1992) 13244.
[25] J.P. Perdew, K. Burke, M. Ernzerhof, Phys. Rev. Lett. 77 (1996) 3865.
[26] H.J. Monkhorst, J.D. Pack, Phys. Rev. B 13 (1976) 5188.
[27] F.D. Murnaghan, Proc. Natl. Acad. Sci. USA 30 (1994) 5390.
[28] J.R. Morris, Y. Ye, Y.B. Lee, B.N. Harmon, K.A. Gschneidner jr, A.M. Russel, Acta Matt. 52 (2004) 4849.
[29] W. Assmus, R. Takke, Sommer, B. Lüthi, J. Phys. C: Solid State Phys 11 (1978) L575.
[30] Y.L. Page, P. Saxe, Phys. Rev. B 63 (2001) 174103.
[31] R.A. Johnson, Phys. Rev. B 37 (1988) 3924.
[32] D.G. Pettifor, Mater. Sci. Technol. 8 (1992) 345.
[33] B. Mayer, H. Anton, E. Bott, M. Methfessel, J. Sticht, P.C. Schmidt, Intermetallics 11 (2003) 23.
[34] S.F. Pugh, Philos. Mag. 45 (1954) 823.
[35] K. Lau, A.K. McCurdy, Phys. Rev. B 58 (1998) 8980.
[36] M. Friák, M. Sob, V. Vitek, Philos. Mag. 83 (2003) 3259.
[37] W. Koster, H. Franz, Metall. Rev 6 (1961) 1.
[38] MH. Ledbetter, in: R.P. Reed, A.F. Clark (Eds.), Materials at low temperatures, American Society for Metals, Metals Park, OH, 1983, p. 1.
[39] S.Q. Wang, H.Q. Ye, Phys. Stat. Sol. (B) 240 (2003) 45.
[40] V. Tvergaard, J.W. Hutchinson, J. Am. Ceram. Soc. 71 (1988) 157.